A&A 390, 1171–1176 (2002)
DOI: 10.1051/0004-6361:20020404

Astronomy & Astrophysics

Integrated optics for astronomical interferometry

V. Extension to the *K* band

E. Laurent[1,2,3], K. Rousselet-Perraut[1], P. Benech[2], J. P. Berger[4,1], S. Gluck[5], P. Haguenauer[1], P. Kern[1], F. Malbet[1], and I. Schanen-Duport[2]

[1] Laboratoire d'Astrophysique de l'Observatoire de Grenoble, BP 53, 38041 Grenoble Cedex 9, France
[2] Institut de Microélectronique, Electromagnétisme et Photonique, BP 257, 38016 Grenoble Cedex 1, France
[3] Alcatel Space Industries, BP 99, 06156 Cannes La Bocca Cedex, France
[4] Harvard-Smithsonian Center for Astrophysics, 60 Garden Street, Cambridge, MA 02138, USA
[5] Laboratoire d'Electronique, de Technologie et de l'Information, 17 rue des Martyrs 38054 Grenoble Cedex 9, France

Received 20 December 2001 / Accepted 14 March 2002

Abstract. We report laboratory and on sky characterizations of planar integrated optics beam combiners in the *K* ([2.0 μm; 2.4 μm]) and *K′* ([2.02 μm; 2.30 μm]) bands. Because of the strong scientific interests of the *K* band, we have extended the integrated optics technologies available in the telecom range (i.e. at 0.8 μm, 1.3 μm and 1.5 μm) to 2.0–2.5 μm. Ion exchange components optimized for these atmospheric bands provide stable contrasts higher than 95% with a laboratory white-light source and global throughputs of 35% in this spectral range. These results are completed with first stellar interferograms obtained with a silica-on-silicon two-way beam combiner on the IOTA interferometer. We characterized in the *H* and *K* bands the throughput of this beam combiner optimized for the *H* band ([1.47 μm; 1.78 μm]). On-sky fringes obtained on ιAur in the *H* and *K′* bands clearly demonstrate a high instrumental contrast (larger than 50%) in both bands. This shows that integrated optics works with high performance outside its usual wavelength domain and provides good solutions for astronomical interferometry in a large wavelength range. We have measured single-mode ranges over 1 μm on our components which would allow to observe in two spectral bands simultaneously or to integrate both metrology reference and science signals in a single chip for astrometric applications.

Key words. techniques: interferometric

1. Introduction

Spatial filtering by guided optics is an important issue to drastically improve the accuracy of the visibility measurements. This principle is applied since 1991 (Coudé du Foresto et al. 1991) by several teams: fluoride directional couplers for the FLUOR beam combination on the IOTA interferometer (Perrin et al. 1999), a single fluoride-glass fiber for spatial filtering on the Palomar Testbed Interferometer (Colavita et al. 1999), or a fluoride fiber beam combiner for the VINCI commissioning instrument of the European Very Large Telescope Interferometer (Glindemann et al. 2001). These experiments operate around 2 μm where scientific interests are strong and coupling efficiency is increased under turbulent atmospheric conditions with respect to shorter wavelengths (Coudé du Foresto et al. 2000).

Kern et al. (1996) has suggested to combine interferometric beams with planar integrated optics (IO) components to take benefit of spatial filtering, stability and compactness. Beam combiners have been manufactured by photolithographic techniques: either by exchanging ions inside a planar glass substrate (Schanen-Duport et al. 1996) or by etching doped silica layers on a silicon substrate (Mottier 1996). Both technologies are industrially mature in the telecom and microsensor fields for the 0.8 μm, 1.3 μm and 1.5 μm wavelengths and can thus be directly used for astronomical applications in the *I*, *J* and *H* atmospheric bands. Several laboratory characterizations (Berger et al. 1999; Haguenauer et al. 2000; Severi et al. 2001) and first stellar observations (Berger et al. 2001) with two-telescope beam combiners have allowed to validate this approach in the atmospheric *H* band.

The lack of telecom or metrology application at 2 μm does not lead to technological developments at these wavelengths. But our encouraging results in the *H* band and the intrinsic glass and silica throughputs up to 2.5 μm lead us to develop integrated optics components dedicated to the *K* band. We manufacture two sets of ion-exchange beam-combiners whose exchange times are adapted to the *K* band (Sect. 2). Throughput (Sect. 3), single-mode behavior (Sect. 4) and laboratory interferometric characterizations (Sect. 5) of these optimized components are analyzed in details. This work is completed by the

Send offprint requests to: E. Laurent,
e-mail: Emmanuel.Laurent@obs.ujf-grenoble.fr

first observations carried out in the H and K' bands on the IOTA interferometer with a silica-on-silicon beam combiner. The latter is optimized for the H band but given the intrinsic throughput of silica, we try in the technical run (Berger et al. 2001) to record flux and fringes in the K' band as a test in real conditions (Sect. 6). Perspectives for broad band single-mode components are finally discussed in Sect. 7.

2. Manufacturing K band components

2.1. Ion-exchange components

The manufacturing process of K band components by ion-exchange technology is the same as for H band (Malbet et al. 1999). The Na^+ ions of the glass substrate are exchanged, through a window, by diffusion process with Ag^+ ions of a molten salt. The local increase of the refractive index is around 0.01 (the refractive index of the used glass is 1.49 at 1.5 μm). The window is made by classical photo-masking techniques.

The GeeO[1] silica customed glass used for Na^+/Ag^+ ion-exchange is optimized for manufacturing waveguide at 1.55 μm. The spectral transmission of this glass (Fig. 1) have an upper spectral limit around 2.7 μm due to OH absorption bands, as well known in fiber manufacturing. The mean intrinsic losses of this material in the K band is 0.5 dB/cm to be compared to 0.09 dB/cm in the H band.

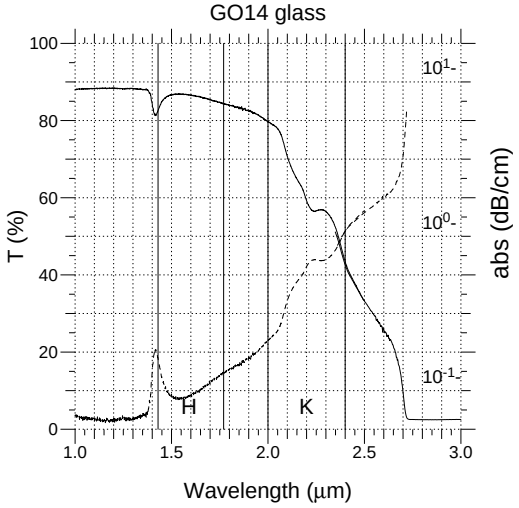

Fig. 1. Intrinsic transmission (where Fresnel losses have been divided) of a 3.4 cm thick glass substrate in the H and K bands (solid line and left axis) and the corresponding absorption curve (dashed and right logarithmic axis).

Manufacturing parameters of the H band component need to be adapted for the K band to obtain larger wave- guides or to adapt the refractive index profile. For this first run we choose to increase the exchange time and to keep the exchange temperature unchanged. GeeO manufactured two sets of components with different exchange times.

Each set of components includes straight waveguides and beam combiners. The design of the two-telescope beam combiners is identical to those characterized in the H band by Berger et al. (1999) and Haguenauer et al. (2000). They include a reverse Y-junction for beam combination and two photometric outputs to calibrate the intensity fluctuations (Fig. 2 left). We have not tested ion-exchange K band beam combiners on the sky because there were not available at the time of the observing run.

[1] Company at Grenoble, France.

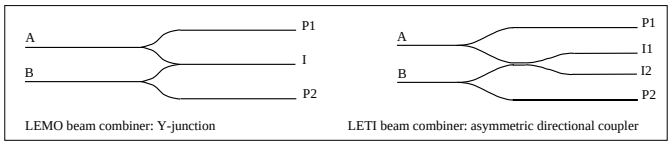

Fig. 2. Schematic view of beam combiners. The inputs are at left and the outputs are at right. I_x and P_x denote interferometric and photometric outputs respectively. Two beam combiners in two technologies are presented: the Y-junction in the ion-exchange LEMO technology (left) and the coupler in the LETI silica-on-silicon technology (right).

2.2. Silica-on-silicon components

Doped silica layers of various refractive index are etched in the areas defined by a mask, leading to index variations from 0.003 to 0.5 (Mottier 1996). Until now we have not modified the technological parameters but we used H band custom components in the K band since doped silica is transparent in this band. The two-telescope beam combiner tested on the sky includes an asymmetrical directional coupler for beam combination and two photometric outputs (Fig. 2 right). The waveguide widths (~5 μm) in the coupling region are not the same in the two arms in order to adapt the coupling rate throughout a wide spectral range. To match technological parameters to manufacture K band components we could modify the width of the mask window, the layer thickness or the doped level.

3. Throughput measurements

3.1. Instrumental set-up and data reduction

A broad band light source is coupled through a K band astronomical filter in the component via a single-mode fiber (Fibercore polarization-maintaining silica fiber whose cut-off wavelength is close to 1.9 μm).

The waveguide outputs are imaged with a microscope objective onto a camera. The flux normalization was achieved by measuring the power directly at the output of the fiber. By injecting in the different inputs, we could deduce the different loss origins. Propagation losses ($P_{\rm prop}$) are deduced from measurements on straight waveguides. Fresnel losses ($P_{\rm fr}$) due to glass/air reflections are calculated from the glass refractive index. Coupling losses ($P_{\rm coupl}$) due to the difference between fiber and waveguide mode diameters are estimated by imaging these modes and by computing the maximal coupling.

Table 1. Estimation of optical losses at different levels of the ion-exchange beam combiner in the K band ([1.98 μm; 2.48 μm]). The number of detected and estimated output photons are given for our 4-cm component and for 100 photons in each input beam. For comparison, last column gives the losses obtained in the H band for the same Ag^+ design component (Haguenauer et al. 2000). The actual H band component have a better throughput with the design improvement on curvatures and Y-junction angles (unpublished measurements).

Band	K	H
Experimental throughput	35%	43%
Theoretical throughput	40%	46%
Propagation losses	42%[a]	9% [b]
Fresnel losses	4%	4%
Coupling losses	7%	20%
Combination losses[c]	50%	50%
Function losses	10%	10%
Number of input photons	200	200
Detected photons	70	86

[a] ~0.5 dB/cm for a total length of 4 cm.

[b] ~0.1 dB/cm for a total length of 4 cm.

[c] 50% of the flux in a reverse Y-junction is radiated out (Malbet et al. 1999).

3.2. Ion-exchange components

The ion-exchange component design involves combination losses ($P_{\rm comb}$) of 50% due to the reverse Y-junction. Functionnal losses ($P_{\rm func}$) due to Y-junctions and bends are deduced from the transmission equation of the component:

$$T = (1 - P_{\rm prop})(1 - P_{\rm fr})(1 - P_{\rm coupl})(1 - P_{\rm func}) \\ *(0.5 + 0.5(1 - P_{\rm comb})). \quad (1)$$

Theoretical throughputs assuming null functional losses are computed to give an upper limit of component throughputs. The throughput comparison between a H band optimized component and a K band one clearly shows that the main difference is the higher propagation losses in the K band (Table 1). In each band, propagation losses are close to the bulk losses (Sect. 2) and could not be improved except by changing the technology (changing the glass or the exchanged ions for example). So future improvements can be foreseen essentially at the design level, on curvatures and/or combination designs. These improvements do not depend on the spectral range and can directly be applied for the K band, which allows to contemplate future K-band two-telescope beam combiners with throughputs higher than 50%.

3.3. Silica-on-silicon components

The tested two-telescope component (Fig. 2 right) is connected with highly-birefringent fibers whose cut-off wavelength is around 1.3 μm since it is dedicated to the H band. The throughput of the fibered component is of 44% in the H band and of 16% in the K' band. Complementary measurements at 1.58 μm on other chips (with an identical design but without fiber connectorization) lead to throughputs as high as 78%. This indicates that the fiber-component coupling is not optimal (fiber losses are much smaller than coupling losses). For the K band, technological parameters of the components have obviously to be adapted and dedicated K band fibers need to be used.

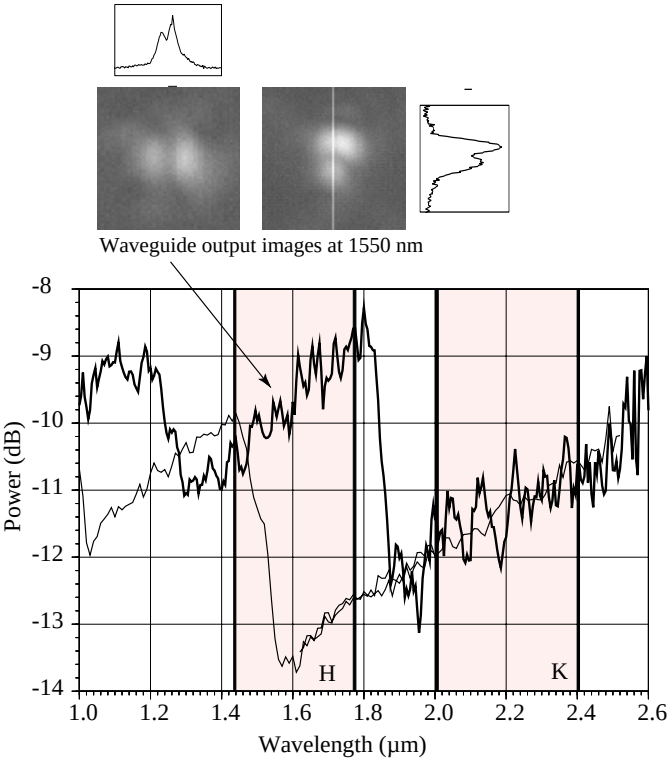

Fig. 3. Typical normalized spectra of the ion-exchange waveguides in the near-infrared. The spectra are computed with the relation $P = 10.\log_{10}(F_{\rm wg}/F_{\rm mm})$ where $F_{\rm wg}$ refers to the spectra with the waveguide and $F_{\rm mm}$ to the spectra with two multimode fibers only. The thiner curve refers to a waveguide with a single-mode limit at 1.55 μm and the thicker curve to a waveguide with a single-mode limit at 1.85 μm. This last waveguide is thus bimode at 1.55 μm, as illustrated by the waveguide output images (in the upper). These outputs are obtained by selectively exciting the second waveguide mode.

4. Single-mode range

One of the main interest of using guided optics in stellar interferometer is the spatial filtering which increases measurement accuracy (Coudé du Foresto et al. 1997). Spatial filtering is obtained thanks to single-mode propagation in waveguides whose behavior is intrinsically chromatic. A symetrical waveguide is single-mode at all wavelengths higher than the cut-off one, provided that the material remains transparent. But in practice, the single-mode behavior with the wavelength is limited by waveguide geometrical imperfections and by the spreading out of the Gaussian mode as the wavelength increases.

We characterized the single-mode behavior of our ion-exchange components by exciting all the waveguide modes with a broad band source coupled to a multimode fiber and by spectrally analyzing the flux at the waveguide output coupled to another multimode fiber. We normalized the spectra with that obtained when the two multimode fibers are coupled (Fig. 3).

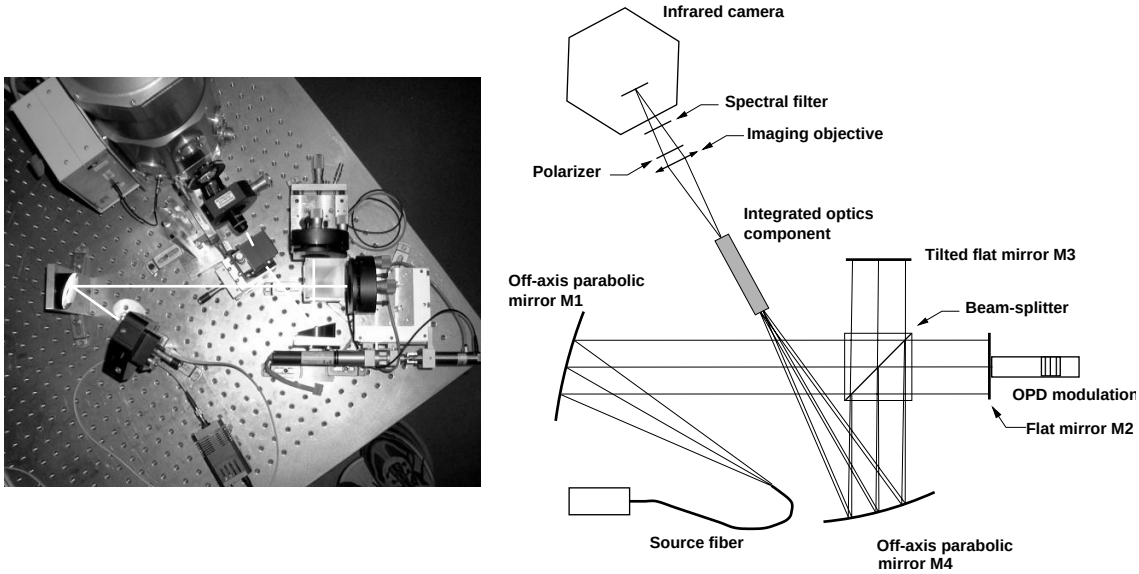

Fig. 4. Laboratory interferometric testbench for measuring instrumental contrasts of planar integrated optics two-telescope beam combiners (see text for details).

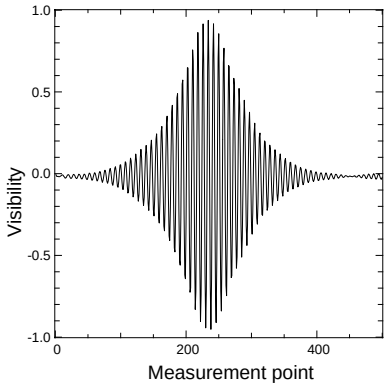

Fig. 5. Corrected white light interferogram at 2.0 μm obtained with a dedicated ion-exchange two-telescope beam combiner. The Gaussian fringe enveloppe is due to the spectral set-up throughput centered at 2030 nm with a $FWHM$ of 90 nm.

Each "bump" is the signature of the loss of one guided mode. One waveguide is single-mode from 1.85 μm to at least 2.6 μm (thick curve). The upper limit is imposed by the low global throughput of the measurement device and not by the waveguide itself. The next "bump" is the bi-mode/single-mode limit. The other waveguide is single-mode from 1.55 μm (thin curve). By adjusting the exchange time, we have well adapted the component single-mode range.

5. Contrast measurements with K-band dedicated ion-exchange components

We have set up a dedicated test bench to inject light into the two waveguides of the beam combiner without fibers. This allows to characterize the interferometric behavior of the component alone. Light provided by a fibered white light source and collimated by the off-axis parabola M1 is splitted in two beams (Fig. 4). In this Michelson arrangement, the 2 beams are reflected by 2 flat mirrors (M2 and M3). One of them is tilted to generate two distinct spots that are focused on the two input waveguides of the IO component thanks to the M4 off-axis parabolic mirror. The M2 flat mirror is mounted on a piezo-electric actuator to modulate the optical path difference (OPD) for temporally scanning of the interferograms. The set-up is completely described in Haguenauer (2001). For our measurements, we use a K band astronomical filter and a K band single-mode fiber as source fiber (the same described in Sect. 3.1).

We use the same acquisition mode as Berger et al. (1999) and contrasts of 95% have been obtained on ion-exchange components (Fig. 5). The interferogram envelope is nearly Gaussian due to the spectral throughput of the set-up in the K band. A Fourier transform of interferograms performed without component shows us that the spectral throughput is a sharp Gaussian centered at 2030 nm with a $FWHM$ of 90 nm. which explains the large number of fringes. The set-up throughput does not cover all the K band probably because the optics (beam-splitter and imaging objective) are not optimized for the K band.

The contrast stability is better than ±0.5% over 10 successive interferograms. A contrast improvement of 1%–3% is measured with linearly polarized incident light. The analysis of the phase difference versus wavelength for several interferograms obtained with the piezoelectric OPD modulation shows that chromatic dispersion inside the ion-exchange component is not detectable with the method detailed by Haguenauer et al. (2000). This confirms that polarization and chromatic effects of the components are small enough to not dramatically degrade the instrumental contrast.

6. First results on the IOTA Interferometer with a silica-on-silicon component

Berger et al. (2001) reports the first interferometric observations of stars using integrated optics beam combiners on the IOTA interferometer (Traub 1998). IOTA is a two-telescope interferometer with a 38 meters maximum baseline, 45 cm

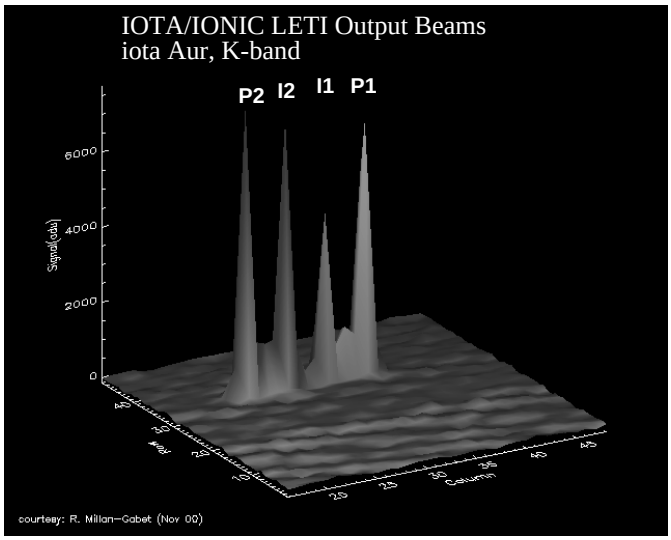

Fig. 6. Image of the four outputs of the silica-on-silicon two-way beam combiner obtained with the IOTA Nicmos camera in the K' band. The lateral spots correspond to the photometric outputs ($P1$, $P2$) and the central ones to the interferometric outputs ($I1$, $I2$) of the directional coupler. The structures that appear between the main spots are due to light propagation between substrate and core of the waveguides which are partially etched (Mottier 1996). *Courtesy: R. Millan-Gabet (Nov. 2000).*

collectors and optimized for the J, H and K' bands. During this run, we have tested the silica-on-silicon coupler in the H and K' bands. Figure 6 shows an image of the component outputs obtained with the IOTA Nicmos infrared camera in the K' band.

We recorded fringes on ιAur in both bands at the projected baseline of 25 m (Fig. 7). Each observation consists of a background measurement and a set of 100 scans of the OPD performed with a piezo-actuated mirror in one interferometer arm. The simultaneous acquisitions of the interferograms and of the photometric signals are synchronized with the piezoelectric displacement. The data reduction procedure is detailed in Berger et al. (2001). The raw visibilities ($V_{\rm raw}$) as well as their corresponding error are the averages and the standard deviations of five (three in K' band) visibilities measured on five (three in K' band) batches of 100 interferograms. These raw visibilities, corrected for photometric signals, correspond to the product of the object visibility and of the instrumental visibility of IOTA and IO component (Table 2). As we did not have a calibrator object to measure the latter, we computed the theoretical visibility of ιAur from his known angular diameter. If we adopt a ιAur angular diameter of 6.3 ± 0.6 mas (Dyck et al. 1998) in the H and K' bands, we can deduce the IOTA-IO instrumental contrast: it exceeds 65% in the K' band while it is of the order of 50% in the H band. These values agree well with the fact that instrumental contrast is more degraded by atmospheric turbulence in the H band than in the K one.

7. Discussion and conclusion

We have obtained first high-constrast white-light interferograms with two-way planar optics beam combiners operating

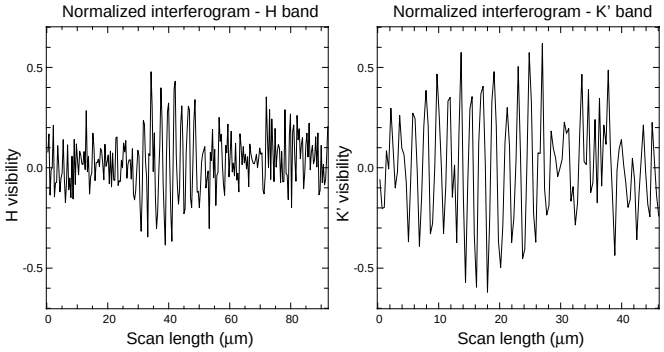

Fig. 7. Typical normalized interferograms obtained on ιAur with a silica-on-silicon beam combiner with the IOTA Interferometer in the H band (left) and in the K' band (right). The projected baseline equals 25 m.

Table 2. ιAur observations in H and K' bands at projected baselines B. Raw visibilities ($V_{\rm raw}$), corrected from photometric signals, correspond to the object and the instrumental visibility. The instrumental visibility of IOTA and IO component $V_{\rm iota+io}$ is deduced from the ιAur angular diameter.

Source	ιAur	
band	K'	H
λ (μm)	2.16	1.65
B (m)	25.4	25.2
$V_{\rm raw}$	0.58 ± 0.02	0.30 ± 0.02
$V_{\rm iota+io}$	0.65	0.50

in the K band. The high and stable contrasts as well as the satisfying optical throughput demonstrate that the available technologies of ion exchange and silica-on-silicon etching can be directly applied in the K band. For both techniques, technological parameters should nevertheless be optimized as we demonstrated with the ion-exchange component. These encouraging results are also confirmed by IOTA observations in the H and K' bands with the same silica-on-silicon single-mode beam combiner.

For both technologies, the throughputs could be improved on the fiber/guide coupling and on the beam combiner design. For wavelengths above 2.5 μm silica glass is not transparent and new technologies have to be investigated to manufacture single-mode waveguides (Laurent et al. 2000).

Single-mode ranges over 1000 nm have been measured on our components. Both technologies can thus provide very broad spectral band components, at least for operating in the H and K bands simultaneously. By changing the spectral filter, we could easily change the observation spectral band during the same night as clearly shown by Berger et al. (2001). We could also separate the spectral bands by using a bulk dichroic at the IO chip output or by using a dichroic function on the chip (Magerand et al. 1994; Mestric et al. 1996). For this purpose, using off-axis parabola for light injection in components is an attractive solution to overcome the limited single-mode range of the injection fibers. In addition to these spectral opportunities, broad single-mode ranges allow to foresee more complex components including on a single chip metrology reference and science signals for astrometry and fringe tracking devices.

Acknowledgements. This work was partially funded by the French spatial agency CNES and by the CNRS/INSU. The integrated optics components have been manufactured and/or fiber-connected by the GeeO company and by the CEA/LETI at Grenoble (France). The authors are grateful to the group of Pascale Berruyer (CEA/LETI/DTS) for the fruitful discussion on LETI technology. We would like to thank Jean-Emmanuel Broquin from IMEP for valuable discussions about single-mode waveguide behavior. The authors are also grateful to Robert Romestain of the LSP, Laboratoire de Spectrométrie Physique at Grenoble in France and to Michel Langlet of the LMGP, Laboratoire des Matériaux et Génie Physique at Grenoble in France for the access to the IR spectrometers. We also thanks Francois Reynaud at IRCOM, Institut de Recherche en Communications Optiques et Microondes in France for the Fibercore fiber and Rafael Millan-Gabet for the kind support at IOTA.

References

Berger, J.-P., Rousselet-Perraut, K., Kern, P., et al. 1999, A&AS, 139, 173

Berger, J.-P., Haguenauer, P., Kern, P., et al. 2001, A&AS, 376, L31

Colavita, M. M., Wallace, J. K., Hines, B. E., et al. 1999, ApJ, 510, 505

Coudé du Foresto, V., Faucherre, M., Hubin, N., & Gitton, P. 2000, A&AS, 145, 305

Coudé du Foresto, V., Perrin, G., Ruilier, C., et al. 1998, Proc. SPIE, 3350, 856

Coudé du Foresto, V., Ridgway, S., & Mariotti, J.-M. 1997, A&AS, 121, 379

Coudé du Foresto, V., & Ridgway, S. 1991, ESO Conf. 15-18 Oct. 1991

Dyck, H. M., Van Belle, G. T., & Thompson, R. R. 1998, AJ, 116, 981

Glindemann, A., Bauvir, B., Delplancke, F., et al. 2001, The Messenger, 104, 2

Haguenauer, P., Berger, J. P., Rousselet-Perraut, K., et al. 2000, Appl. Opt., 39, 13, 2130

Haguenauer, P. 2001, Ph.D. Thesis

Kern, P., Malbet, F., Schanen-Duport, I., & Benech, P. 1996, in Proc. AstroFib'96, Integrated Optics for Astronomical Interferometry, ed. P. Kern, & F. Malbet (Bastianelli-Guirimand, Grenoble), 195

Laurent, E., Schanen, I., Malbet, F., & Taillades, G. 2000, Proc. SPIE, 4006, 1090

Magerand, J., Grand, G., Pouteau, P., & Philippe, P. 1994, Proc. SPIE, 2213, 228

Malbet, F., Kern, P., Schanen-Duport, I., et al. 1999, A&AS, 138, 135

Mestric, R., Bissessur, H., Martin, B., & Pinquier, A. 1996, IEEE Photonic Technol. Lett., 8, 5

Mottier, P. 1996, in Proc. AstroFib'96, Integrated Optics for Astronomical Interferometry, ed. P. Kern, & F. Malbet (Bastianelli-Guirimand, Grenoble), 63

Ochsenbein, F., & Halbwachs, J. L. 1982, A&AS, 47, 523

Perrin, G., Coudé du Foresto, V., Ridgway, S., et al. 1999, A&A, 345, 221

Ridgway, S., Joyce, R., White, N., & Wing, R. 1980, ApJ, 235, 126

Richichi, A., Ragland, S., Stecklum, B., & Leinert, C. 1998, A&A, 338, 527

Schanen-Duport, I., Benech, P., Kern, P., & Malbet, F. 1996, in Proc. AstroFib'96, Integrated Optics for Astronomical Interferometry, ed. P. Kern, & F. Malbet (Bastianelli-Guirimand, Grenoble), 99

Severi, M., Haguenauer, P., Rousselet-Perraut, K., et al. 2001, Appl. Optics, submitted

Traub, W. 1998, Proc. SPIE, 3350, 848